Journal Pre-proofs

Research paper

Kinetically unstable 2–isocyanophenol isolated in cryogenic matrices: Vibrational excitation, conformational changes and spontaneous tunneling

A.J. Lopes Jesus, Igor Reva, Cláudio M. Nunes, José P.L. Roque, Sandra M.V. Pinto, R. Fausto

Please cite this article as: A.J. Lopes Jesus, I. Reva, C.M. Nunes, J.P.L. Roque, S.M.V. Pinto, R. Fausto, Kinetically unstable 2–isocyanophenol isolated in cryogenic matrices: Vibrational excitation, conformational changes and spontaneous tunneling, *Chemical Physics Letters* (2019), doi: https://doi.org/10.1016/j.cplett. 2019.137069

This is a PDF file of an article that has undergone enhancements after acceptance, such as the addition of a cover page and metadata, and formatting for readability, but it is not yet the definitive version of record. This version will undergo additional copyediting, typesetting and review before it is published in its final form, but we are providing this version to give early visibility of the article. Please note that, during the production process, errors may be discovered which could affect the content, and all legal disclaimers that apply to the journal pertain.
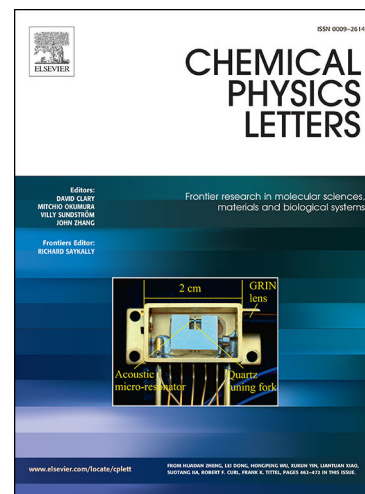
Kinetically unstable 2-isocyanophenol isolated in cryogenic matrices: vibrational excitation, conformational changes and spontaneous tunneling

A. J. Lopes Jesus,[a,b] Igor Reva,*[a] Cláudio M. Nunes,[a]

José P. L. Roque,[a] Sandra M. V. Pinto,[a,†] and R. Fausto[a]

[a] *CQC, Department of Chemistry, University of Coimbra, 3004-535, Coimbra, Portugal.*
[b] *CQC, Faculty of Pharmacy, University of Coimbra, 3004-295, Coimbra, Portugal.*

_____

* Corresponding author. *E-mail address*: reva@qui.uc.pt
† Present address: Scuola Normale Superiore, Piazza dei Cavalieri, 7, I-56124 Pisa, Italy.

Abstract

Monomers of 2-isocyanophenol were generated in low-temperature solid Ar and N_2 matrices by UV-irradiation of benzoxazole and characterized by infrared (IR) spectroscopy. Near-IR narrowband excitation of the first OH-stretching overtone of 2-isocyanophenol isolated in an N_2 matrix converted the most stable *cis* into the higher-energy *trans* conformer. Interconversions between these conformers also occurred when the sample was vibrationally excited by the full, or filtered, broadband light of the spectrometer source, notably, with different isomerization rate constants. A spontaneous *trans* $\rightarrow$ *cis* decay, *via* H-tunneling, was observed for N_2 matrix kept in dark. In an Ar matrix, only the *cis* conformer was observed.

1. Introduction

The method of matrix isolation was first developed in 1954, by the groups of Porter [1] and Pimentel [2] with the purpose of studying short-lived reaction intermediates. In the early sixties, Pimentel *et al.* reported isomerization of nitrous acid (HONO) [3,4] as a result of an "Infrared Chemical Reaction" induced by broadband light emitted by the infrared spectrometer light source. After these reports, the infrared-induced chemistry of matrix-isolated molecules was barely explored over the course of three decades. However, the seminal work of Pettersson, Lundell, Khriachtchev and Räsänen [5] rekindled interest to this topic in 1997. Monomers of the most stable conformer (*cis* with respect to the OCOH dihedral) of formic acid (HCOOH) isolated in an Ar matrix were vibrationally excited by narrowband near-infrared (NIR) light tuned at the frequency of the observed first OH stretching overtone (6934 cm^{-1}) [5]. This resulted in generation and spectroscopic characterization of the elusive *trans* OCOH conformer. They also found that, in an Ar matrix at 15 K, the higher energy *trans* conformer, once generated, converted back to the most stable *cis* form on a time scale of minutes, *via* hydrogen tunneling [5]. A few years later, in 2000, Khriachtchev *et al.* have revisited the IR-induced chemistry of matrix-isolated HONO [6]. They performed NIR laser irradiation of the matrix-isolated molecules of the compound at the frequency of the first OH and N=O stretching overtones of each conformer, which resulted in selective *trans→cis* or *cis→trans* conformational isomerization, depending on the conformer being excited. Noteworthy, these processes were found to be selective not just to a specific conformer but even with respect to the matrix sites, showing the great potential of the narrowband vibrational excitations in promoting infrared-induced conformational changes [6].

Spontaneous tunneling of *trans* formic acid generated *in situ* by NIR excitation of the *cis* conformer (as described above) was investigated in detail in different noble gas matrices (Ar, Kr, Xe) and it was found that the medium has a significant influence on the tunneling rate (within the half-lives of minutes) [7]. Rotational isomerization of other small carboxylic acids isolated in noble gases matrices was studied using the same approach, with focus on photoinduced generation of higher energy conformers and tunneling [8,9]. The state-of-art of preparation of higher-energy conformers by selective vibrational excitation was reviewed by Khriachtchev in 2008 [10].

The next breakthrough in the field started with two simultaneous publications [11,12], both authored by Khriachtchev *et al.* It was recognized that in N$_2$-doped Ar matrices [11], as well as in neat N$_2$ matrices [12], the lifetimes of the higher-energy conformers of formic and

acetic acids increase by one or two orders of magnitude, approaching several hours [11,12]. This finding opened up the door for application of steady-state spectroscopic methods for characterization of elusive high-energy conformers of many chemical systems otherwise not amenable to experiment, after their generation in N_2 matrices.

In the examples reported above, the higher-energy elusive conformers were generated using commercially available precursor compounds. Recently, we have been using another approach, whereby the high-energy kinetically unstable compounds are generated directly in the cryogenic matrix, being subsequently used as targets for conformational manipulations. In such a way, we have UV-generated (λ = 224 nm) *in situ* the elusive hydroxy- or amino-derivatives of 2-formyl-2*H*-azirines from the respective isoxazole precursors in Ar matrices at 15 K (see Fig. 1 for the hydroxy-derivative). Once formed, the conformational isomerization of the formyl group in these azirines was successfully promoted by vibrational excitations of the first OH or NH_2 stretching overtones [13]. In another study, we started with the commercially available thioacetamide, which exists exclusively in its conformationally rigid amino-thione tautomer $S=C(CH_3)-NH_2$. Using UV-excitations (λ = 265 nm), four high-energy (38 kJ mol^{-1} or more with respect to the thione isomer) imino-thiol isomers $H-S-C(CH_3)=N-H$, differing by mutual orientations of the SH and NH groups, were generated [14,15]. This allowed for subsequent studies of spontaneous [14] and vibrationally-induced (by excitation of the first NH stretching overtones) [15] conformational isomerizations.

In the present work, we report on the UV-induced generation of kinetically unstable 2-isocyanophenol (**2**) from commercially available benzoxazole (**1**) isolated in cryogenic Ar and N_2 matrices. In N_2 matrices, it was possible to trap two conformers of **2** and study their mutual transformations, both light-induced and spontaneous. These experiments allowed for the structural and vibrational characterization of the two conformers of 2-isocyanophenol, which are reported here for the first time.

2. Experimental and computational methods

Commercial benzoxazole (**1**) (TCI Europe, > 98%) was used in the present study as the starting material. The compound was placed in a glass ampoule, connected to the cryostat via SS-4BMRG (NUPRO) needle valve with a shut-off and metering possibility. Prior to the experiment, the cell with benzoxazole was connected to the vacuum system of a closed-cycle helium refrigerator (APD Cryogenics, with a DE-202A expander) and the compound was additionally purified from volatile impurities by pumping through the cryostat. Matrices were

prepared by simultaneous condensation of benzoxazole with a large excess of inert gas (argon N60 and nitrogen N50, both supplied by Air Liquide) onto a cryogenic CsI window (~15 K) which was used as optical substrate. The sublimation rate of benzoxazole was chosen to be low enough to ensure that the species trapped in the matrices were mainly monomers. For this purpose, during sublimation, crystals of benzoxazole were cooled to 0 °C by immersing the ampoule with the compound into a bath with melting water-ice mixture. This allowed to reduce the saturated vapor pressure over the compound and to improve the metering function of the needle valve. A glass vacuum system and standard manometric procedures were applied to deposit the matrix gas (Ar or N_2), from a separate inlet port.

The compound of interest, 2-isocyanophenol (**2**), was photogenerated *in situ* by irradiating matrix-isolated **1** with UV-light at $\lambda = 233$ nm (absorption maximum of **1** in ethanol [16]). After photogeneration of **2**, irradiations were also performed in the near-infrared (NIR) region. Monochromatic (full width at half-maximum ~0.2 cm^{-1}) UV or NIR light was provided by a frequency-doubled signal or idler beam, respectively, of a Quanta-Ray MOPO-SL pulsed optical parametric oscillator (pulse duration 10 ns, repetition rate 10 Hz). The pulse energy used was 0.5 mJ (UV) or 8 mJ (NIR).

FTIR spectroscopy was used for vibrational characterization of the trapped species and also for following their light-induced and spontaneous transformations. In some experiments, a standard Edmund Optics longpass filter was used (transmission cut-off value of ~4.50 μm) to protect the sample from infrared light with wavenumbers above ~2200 cm^{-1}. Other details of the experimental setup and methodology used in the matrix deposition, UV and NIR irradiations and acquisition of IR spectra, have been described elsewhere [17].

All theoretical calculations were performed with the Gaussian 09 software package (Revision D.01) [18]. The geometries of two conformers of **2**, and the transition state between them, were optimized using the B3LYP [19-21] and MP2 [22] methods, combined with the 6-311++G(d,p) and 6-311++G(3df,3pd) basis sets [23-25], respectively (Cartesian coordinates of the optimized geometries are listed in Table S1). Harmonic vibrational calculations at both levels were carried out for the respective optimized geometries. The nature of stationary points as true minima, or first-order transition states, was confirmed by analysis of the corresponding Hessian matrices. The wavenumbers computed for **2** at the B3LYP/6-311++G(d,p) level were subjected to least squares linear fit against the experimental wavenumbers observed for the *cis* conformer **2c** in an Ar matrix (see Section **3.2**), resulting in scaling factors of 0.983 or 0.948, below and above 3000 cm^{-1}, respectively. The scaled wavenumbers, and absolute infrared intensities extracted from the B3LYP vibrational calculations, were used to simulate IR spectra.

For this purpose, the peaks centered on the scaled frequencies, were convoluted with Lorentzian functions having a full-width at half-maximum (fwhm) of 1 or 2 cm^{-1} and peak heights equal to the calculated IR intensities.

The theoretical normal modes were analyzed by carrying out potential energy distribution (PED) calculations. Transformation of the force constants with respect to the Cartesian coordinates into the force constants with respect to the molecule-fixed internal coordinates allowed the PED analysis to be carried out as described by Schachtschneider and Mortimer [26]. The set of internal coordinates used in the PED analysis is given in Table S2 and is defined as recommended by Pulay *et al.* [27]. The atom numbering is presented in Fig. S1. The resulting vibrational assignments of the two conformers, including the elements of PED matrices greater than 10%, are presented in Tables S3 and S4. B3LYP anharmonic vibrational computations were also carried out using the fully automated second-order vibrational perturbative theory (VPT2) approach of Barone and co-workers [28-30]. Calculated anharmonic wavenumbers were not scaled.

3. Results and discussion

3.1. Relative stability of the 2-isocyanophenol conformers and energy barriers for their interconversion

2-Isocyanophenol **2** has two planar conformers (C_s symmetry), here denoted as **2c** or **2t**, depending if the hydrogen of the OH group points toward (*cis*, **c**) or away (*trans*, **t**) from the isocyano group (−N≡C), respectively (Table 1). B3LYP/6-311++G(d,p) and MP2/6-311++G(3df,3pd) relative electronic (ΔE_{el}) and zero-point corrected (ΔE_0) energies for the two conformers are given in Table 1. Both methods predict an energy difference (zero-point corrected) between the two forms of ~11 kJ mol^{-1}. The lower energy of **2c** can be rationalized by considering the existence in this conformer of a stabilizing O−H⋯N hydrogen bond-like interaction, as revealed by the geometric parameters given in Table 1, and also by the experimentally observed OH stretching wavenumber redshift of 39 cm^{-1} in **2c** relative to **2t** (Tables S3 and S4). The conformational behaviour of **2** follows the pattern exhibited by other 2-substituted phenols where the substituent acts as a hydrogen bond acceptor [31].

The computed energy barriers for the conformational interconversion ($\Delta\Delta E^{\ddagger}$) are included in Table 1 (the potential energy scan for the internal rotation of the OH group around the C−O bond is shown in Fig. S2). Values of ~22.1 kJ mol^{-1} (~1850 cm^{-1}) and ~11.5 kJ mol^{-1}

6

(~960 cm^{-1}) were obtained for the isomerization in the forward **2c** → **2t** and backward **2c** ← **2t** directions, respectively. A nearly identical OH torsional energy profile has been previously reported for the isomeric 2-cyanophenol molecule (Fig. S2) with forward and backward barriers of 22.0 and 12.4 kJ mol^{-1}, respectively) [32].

3.2. Spectral identification of 2-isocyanophenol and NIR laser induced 2c → 2t conversion

Monomers of benzoxazole **1** were isolated in Ar and N$_2$ matrices and characterized by IR spectroscopy. Some of the strongest bands in the infrared spectrum of **1** isolated in an Ar matrix appear at 1526.5, 1452.6, 1239.3, 1106.0, 1069.8 cm^{-1} (see Fig. S3b). They agree very well with the positions of the strongest bands in the gas phase IR and Raman spectra of benzoxazole, which appear at 1528, 1453, 1238, 1107, 1072 cm^{-1} (reported by Klots and Collier [33]) or at 1523, 1451, 1237, 1105, 1068 cm^{-1} (reported by Mille *et al*. [34]). The experimental values also match well the strongest IR bands computed at the B3LYP/6-311++G(d,p) level: 1535.5, 1450.6, 1233.8, 1105.3, 1061.5 cm^{-1} (Fig. S3c).

Matrix-isolated **1** was subjected to a series of narrowband UV-irradiations at λ = 233 nm. In Ar matrix, these irradiations led to the consumption of **1** and formation of a photoproduct with strong infrared absorptions at 3584 and 2118 cm^{-1} (Fig. 2). Absorptions at such frequencies are typical of OH and −N≡C stretching vibrations. Interestingly, when Ferris *et al.* studied the photochemistry of 1,2-benzisoxazole **3** at −77 and −196 °C with a λ = 254-nm light source in a KBr matrix or neat film [35], they observed a photoproduct "**X**" with absorption at 2130 cm^{-1} due to the −N≡C stretching. According to those authors, this absorption disappeared on warming to 0 °C in dark, giving rise to the intense IR spectrum of benzoxazole **1** [36]. On this basis, the kinetically unstable product "**X**" was assigned to **2** [35,36]. Besides the −N≡C stretching and the OH stretching (at 3350 cm^{-1}), no other absorptions of **2** had been ever reported. Interestingly, when we studied the UV-photochemistry of matrix-isolated **3** (λ = 280 nm), no signs of formation of **2** from **3** were detected [37]. However, in the present work, **2** is generated from **1** (λ = 233 nm) almost exclusively. The reliable assignment of the photoproduct to **2** is based on the experimental observation, for the first time, of all the 18 vibrations that have their predicted counterparts in the 2200–400 cm^{-1} range with IR intensities above 2 km mol^{-1} (see Fig. 2 and Table S3). This also allowed for deriving a scaling factor by least-squares linear fitting of calculated to experimental wavenumbers (Fig. S4), which was used throughout this work.

Comparison of the results obtained in the two matrices (Ar *vs.* N$_2$) revealed a striking difference. In Ar matrix, the IR spectrum of the photoproduct is fully reproduced by the theoretical spectrum predicted for **2c**, while no signs of **2t** were detected (Fig. 2). On the other hand, in N$_2$ matrix, the most intense bands of the photoproduct are nicely reproduced by the theoretical spectrum of **2c**, but a set of new weaker bands also appears at the positions where **2t** is expected to absorb (compare Fig. 2 and Fig 3). For example, two bands due to the OH stretching mode appear in N$_2$ at 3578 (**2c**) and 3617 (**2t**) cm^{-1}. The latter band nicely agrees with the OH stretching frequency of phenol (OH group free of intramolecular interactions) in N$_2$ matrix reported at 3622 cm^{-1} by Khriachtchev et al. [38]. Characteristic is also the doublet near 2120 (**2c**) and 2135 (**2t**) cm^{-1} (Fig. 3), ascribed to the −N≡C stretching vibration, with a predicted wavenumber difference of 17.3 cm^{-1} (see Tables S3 and S4).

In the NIR spectra recorded after UV-induced generation of **2**, absorption bands were identified at 6992 cm^{-1} in Ar matrix, and at 6986 cm^{-1} in N$_2$ matrix (see Fig. S5). These bands are ascribed to the first OH stretching overtone [2ν(OH)] of **2c**, and their experimental positions are in good agreement with the theoretical anharmonic frequency calculated for this transition (7001 cm^{-1}, Fig. S5).

To investigate the possibility of conformational isomerization between **2c** and **2t** by vibrational excitation, we carried out a series of monochromatic excitations at the frequency of the 2ν(OH) absorption identified for **2c**. In the Ar matrix, irradiations at 6992 cm^{-1} did not produce any observable transformation. However, in the N$_2$ matrix, irradiations at 6986 cm^{-1} for about 100 min led to significant changes in the IR spectrum (Fig. 4). The resulting experimental difference IR spectrum compared with the spectra calculated for **2c** and **2t** clearly indicates that excitation of the 2ν(OH) mode of **2c** promotes a decrease of the bands assigned to this conformer and a concomitant increase of the bands assigned to **2t** (Fig. 4). Thanks to these spectral changes, a detailed assignment of the infrared spectra of matrix-isolated **2**, and particularly of the minor **2t** conformer, was carried out (see Table S4).

The lack of observation of **2t** conformer in the Ar matrix, upon the UV or NIR irradiation experiments, is most probably due to occurrence of fast hydrogen tunneling to the most stable **2c** conformer. This behaviour has been observed for a large number of carboxylic acids with conformers differing by 180° rotation of OH group, such as formic [5,7,8], acetic [8,9], propionic [8], and squaric [39] acids, and in a few phenol derivatives [40-42]. On the other hand, when N$_2$ is used as host medium, it is sometimes possible to extend the lifetime of the high energy rotamers, thus permitting their spectroscopic characterization [12,32,39,43,44]. This is also demonstrated here for the case of **2t** conformer. According to Khriachtchev *et al.*,

the increased stability of the high energy conformers in an N_2 matrix is attributed to the formation of specific OH$\cdots N_2$ interactions [11,12,38,45], due to the fact that N_2 molecules have a permanent quadrupole moment (while noble-gas atoms do not have) [38].

3.3. Conformational changes induced by the broadband IR-radiation emitted from the spectrometer

Conformational changes in matrix-isolated molecules can occur also when they are exposed to the IR broadband radiation emitted by the spectrometer source [4,32,46]. To study such changes for **2** in the N_2 matrix, we followed the time evolution of the population of the two conformers during the exposition of the sample to the spectrometer beam (see caption of Fig.5). The kinetic measurements started from two different **2c** : **2t** population ratios in the matrix, near 75 : 25 and 95 : 5. The first ratio was obtained by performing selective NIR excitations at 6986 cm^{-1} as described above, while the second was achieved by letting the sample in dark for 23 hours at a temperature of 11 K. For the matrix with an initial ratio of 75 : 25, the abundance of **2t** was found to decrease with time, while that of **2c** increased (Fig. 5a, closed symbols). After approximately 40 minutes of exposing the matrix to the spectrometer light source, no further changes in the populations of the two conformers were observed, meaning that a stationary state was reached. At this state, the **2c** : **2t** ratio was estimated to be near 88 : 12. For the matrix with an initial 95 : 5 conformational ratio, the abundance of the two conformers evolved in the opposite direction, i.e. **2t** was found to increase with time (see Fig. 5a, empty symbols). When the system has approached the stationary state, the conformational ratio (about 88 : 12) was found to be identical to that observed in the experiment where the initial conformational ratio was 75 : 25.

The above results show that, independent of the initial conformational composition, the system always tends to the same stationary state upon the same broadband irradiation conditions. At this state, the rate of the **2c** $\rightarrow$ **2t** conversion (promoted mostly by excitation of vibration modes lying above the isomerization barrier, computed $\Delta\Delta E^{\ddagger}_0 \sim 1850$ cm^{-1}) matches that corresponding to the **2t** $\rightarrow$ **2c** conversion (induced by excitation of vibrations lying above the isomerization barrier, computed $\Delta\Delta E^{\ddagger}_0 \sim 960$ cm^{-1}, plus the contribution of hydrogen tunneling). By fitting the experimental data shown in Fig. 5a with an exponential equation, $y = a + be^{-(k_{c\text{-}t}+k_{t\text{-}c})t}$, the following rate constants were estimated for the **2c** $\rightarrow$ **2t** ($k_{c\text{-}t}$) and **2t** $\rightarrow$ **2c** ($k_{t\text{-}c}$) processes: $k_{c\text{-}t} = 2.3 \times 10^{-4}$ s^{-1} and $k_{t\text{-}c} = 1.6 \times 10^{-3}$ s^{-1}.

The kinetic measurements were repeated after enriching the N_2 matrix with the less stable **2t** form, but in this case a longpass filter transmitting only IR-light below 2200 cm^{-1} was placed between the sample and the spectrometer in order to prevent excitation of the higher energetic vibrations, particularly the strongly absorbing $\nu(OH)$ modes. The obtained kinetic data, which are represented in Fig. 5b, show that the populations of the two conformers also tend towards a stationary state, with a conformational ratio of about 90 : 10. The following isomerization rate constants were estimated from the exponential fitting: $k_{c-t} = 9.3 \times 10^{-5}$ s^{-1} and $k_{t-c} = 8.5 \times 10^{-4}$ s^{-1}. These rate constants are, respectively, 60 and 47 % lower than those estimated from the kinetic measurements performed without the presence of the filter. It demonstrates that, besides the excitation of the $\nu(OH)$ and other high-frequency modes, excitation of the low energy vibrations (below 2200 cm^{-1}) also plays a significant role in the conformational changes occurring in the presence of broadband IR-radiation. The fact that the reduction of the **2t** $\rightarrow$ **2c** conversion rate, originated by the presence of the filter, is not so pronounced as that observed for the opposite **2c** $\rightarrow$ **2t** conversion, seems to indicate that the first transformation is not solely determined by a photoinduced process, an observation that is in agreement with the **2t** $\rightarrow$ **2c** decay by tunneling discussed in the next section.

Identical kinetic studies were previously performed for 2-cyanophenol isolated in an N_2 matrix and the rate constants corresponding to the *cis* $\leftrightarrow$ *trans* isomerizations were also estimated for the sample exposed to unfiltered and filtered (below 2200 cm^{-1}) broadband IR-radiation emitted from the spectrometer [32]. In this case, the *cis* $\rightarrow$ *trans* and *trans* $\rightarrow$ *cis* isomerization rate constants, resulting from blocking the absorptions above 2200 cm^{-1}, were found to be, respectively, 80 and 68 % lower than those observed for the corresponding unfiltered processes. This represents a much more pronounced reduction of the rate constants than that here reported for 2-isocyanophenol. Such difference can be interpreted in terms of the position of the intense $\nu(NC)$ or $\nu(CN)$ absorptions relative to the filter cut-off frequency ($\sim$ 2200 cm^{-1}). As shown in Fig. S7, for 2-isocyanophenol these absorptions are located at lower wavenumbers (2133 and 2122 cm^{-1}), while for the isomeric 2-cyanophenol molecule they are located at higher wavenumbers (2239 and 2230 cm^{-1}). This means that the presence of the filter allows excitation of the $\nu(-N{\equiv}C)$ modes in 2-isocyanophenol but prevents excitation of the $\nu(-C{\equiv}N)$ modes in 2-cyanophenol. Then, the higher reduction of the isomerization rate constants for 2-cyanophenol as compared to 2-isocyanophenol can be partially ascribed to blocking excitation of the energetic $N{\equiv}C$ stretching mode in the former molecule, and allowing it in the case of **2**.

3.4. Conformational relaxation in dark

As mentioned above, keeping the N_2 matrix at 11 K in dark resulted in a decrease of the population of the less stable **2t** conformer, and a concomitant increase of the population of the most stable **2c** conformer (see Fig. 6 and S6). At such a low temperature, the observed conformational relaxation cannot take place over the **2t** → **2c** barrier ($\Delta\Delta E^{\ddagger}_0$ above 11 kJ mol^{-1}, see Table 1). This transformation should, therefore, be essentially governed by tunnelling of the hydrogen atom [47,48]. This isomerization mechanism was found to play an important role in the conformational relaxation of other matrix-isolated molecules with OH group linked directly to an aromatic ring such as derivatives of phenol [32,40-42] or of cytosine [49,50].

After increasing the amount of **2t** in the N_2 matrix, using the procedure described above, the **2t** → **2c** decay process was followed as a function of time, by recording a few IR spectra in the presence of the filter cutting the IR-radiation above 2200 cm^{-1}. The population decrease of **2t** (and increase of **2c**) is represented in Fig. 7. Fitting the experimental data with a single-exponential function, a rate constant of $k \sim 3.2 \times 10^{-4}$ s^{-1} was estimated for the observed dark process, which corresponds to a half-life time of $t_{1/2} \sim 36$ min. These values are practically coincident with those recently reported by us for the corresponding dark transformation in 2-cyanophenol isolated in a N_2 matrix at 15 K ($k_{t-c} \sim 3.6 \times 10^{-4}$ s^{-1} ; $t_{1/2} \sim 32$ min) [32], where a barrier with nearly identical shape separates the higher from the lower energy rotamer (see Fig. S2), which explains the observation of similar tunneling rates.

Finally, it is of interest to compare the rate constant estimated for the **2t** → **2c** isomerization in dark with the rate constants estimated above for the same isomerization when the matrix is exposed to the spectrometer source. The obtained results show that the tunneling rate represents ∼ 38 % or ∼ 20% of the overall **2t** → **2c** rate process in the presence of filtered or unfiltered broadband IR-light, respectively. Hence, for the matrix exposed to the spectrometer beam, the tunneling rate is a non-negligible contribution to the overall **2t** → **2c** isomerization rate, in agreement also with the results previously reported for 2-cyanophenol [32].

4. Conclusions

Isocyanophenol (**2**) was photochemically produced in low-temperature Ar and N_2 matrices by irradiating benzoxazole (**1**) with UV-light at $\lambda = 233$ nm. In the Ar matrix, only the most stable **2c** rotamer was captured and spectroscopically characterized. In contrast, both **2c**

11

and **2t** rotamers were identified in an N_2 matrix due to the high stabilizing effect of this matrix medium as compared to the noble gas matrix. For 2-isocyanophenol isolated in solid N_2, selective excitation of the $2\nu(OH)$ mode of the **2c** conformer with NIR laser light promoted the **2c** $\rightarrow$ **2t** transformation. The spectral changes resulting from this conversion allowed a detailed assignment of the IR spectra of the two conformers. When the N_2 matrix is exposed to the broadband IR-radiation (unfiltered or filtered) emitted by the spectrometer light source, the conformational distribution always converges to a stationary state. Excitation of low energy vibrational modes (below 2200 cm^{-1}) was found to play an important role in the IR-induced conformational interconversion. Not only photoinduced processes, but also tunneling contributes to the conformational switching in the presence of the spectrometer beam. For a sample maintained in dark, the higher-energy conformer undergoes a spontaneous tunneling conversion into the lower energy conformer, with a half-life time $\sim$ 32 min. Very interestingly, over-the-barrier (IR-induced) and through-the-barrier (hydrogen tunneling) OH rotamerizations were found to occur on the same time scale (half-lives on the order of tens of minutes), as it follows from the values of the obtained rate constants.

12

References

[1] I. Norman, G. Porter, Nature 174 (1954) 508-509.

[2] E. Whittle, D.A. Dows, G.C. Pimentel, J. Chem. Phys. 22 (1954) 1943-1943.

[3] J.D. Baldeschwieler, G.C. Pimentel, J. Chem. Phys. 33 (1960) 1008-1015.

[4] R.T. Hall, G.C. Pimentel, J. Chem. Phys. 38 (1963) 1889-1897.

[5] M. Pettersson, J. Lundell, L. Khriachtchev, M. Räsänen, J. Am. Chem. Soc. 119 (1997) 11715-11716.

[6] L. Khriachtchev, J. Lundell, E. Isoniemi, M. Räsänen, J. Chem. Phys. 113 (2000) 4265-4273.

[7] M. Pettersson, E.M.S. Maçôas, L. Khriachtchev, J. Lundell, R. Fausto, M. Räsänen, J. Chem. Phys. 117 (2002) 9095-9098.

[8] E.M.S. Maçôas, L. Khriachtchev, M. Pettersson, R. Fausto, M. Räsänen, Phys. Chem. Chem. Phys. 7 (2005) 743-749.

[9] E.M.S. Maçôas, L. Khriachtchev, M. Pettersson, R. Fausto, M. Räsänen, J. Am. Chem. Soc. 125 (2003) 16188-16189.

[10] L. Khriachtchev, J. Mol. Struct. 880 (2008) 14-22.

[11] K. Marushkevich, M. Räsänen, L. Khriachtchev, J. Phys. Chem. A 114 (2010) 10584-10589.

[12] S. Lopes, A.V. Domanskaya, R. Fausto, M. Räsänen, L. Khriachtchev, J. Chem. Phys. 133 (2010) 144507 (1-7).

[13] A.J. Lopes Jesus, C.M. Nunes, R. Fausto, I. Reva, Chem. Commun. 54 (2018) 4778-4781.

[14] S. Góbi, C.M. Nunes, I. Reva, G. Tarczay, R. Fausto, Phys. Chem. Chem. Phys. 21 (2019) 17063-17071.

[15] S. Góbi, I. Reva, I.P. Csonka, C.M. Nunes, G. Tarczay, R. Fausto, Phys. Chem. Chem. Phys. 21 (2019) 24935-24949.

[16] R. Passerini, Journal of the Chemical Society (1954) 2256-2261.

[17] C. Araujo-Andrade, I. Reva, R. Fausto, J. Chem. Phys. 140 (2014) 064306 (1-14).

[18] M.J. Frisch, G.W. Trucks, H.B. Schlegel, G.E. Scuseria, M.A. Robb, J.R. Cheeseman, G. Scalmani, V. Barone, B. Mennucci, G.A. Petersson, H. Nakatsuji, M. Caricato, X. Li, H.P. Hratchian, A.F. Izmaylov, J. Bloino, G. Zheng, J.L. Sonnenberg, M. Hada, M. Ehara, K. Toyota, R. Fukuda, J. Hasegawa, M. Ishida, T. Nakajima, Y. Honda, O. Kitao, H. Nakai, T. Vreven, J.A. Montgomery, Jr., J.E. Peralta, F. Ogliaro, M. Bearpark, J.J. Heyd, E. Brothers, K.N. Kudin, V.N. Staroverov, T. Keith, R. Kobayashi, J. Normand, K. Raghavachari, A. Rendell, J.C. Burant, S.S. Iyengar, J. Tomasi, M. Cossi, N. Rega, J.M. Millam, M. Klene, J.E. Knox, J.B. Cross, V. Bakken, C. Adamo, J. Jaramillo, R. Gomperts, R.E. Stratmann, O. Yazyev, A.J. Austin, R. Cammi, C. Pomelli, J.W. Ochterski, R.L. Martin, K. Morokuma, V.G. Zakrzewski, G.A. Voth, P. Salvador, J.J. Dannenberg, S. Dapprich, A.D. Daniels, Ö. Farkas, J.B. Foresman, J.V. Ortiz, J. Cioslowski, D.J. Fox, Gaussian 09. Gaussian, Inc., Wallingford, CT, 2013.

[19] A.D. Becke, J. Chem. Phys. 98 (1993) 5648-5652.

[20] S.H. Vosko, L. Wilk, M. Nusair, Can. J. Phys. 58 (1980) 1200-1211.

[21] C.T. Lee, W.T. Yang, R.G. Parr, Phys. Rev. B 37 (1988) 785-789.

[22] C. Møller, M.S. Plesset, Physical Review 46 (1934) 618-622.

[23] R. Krishnan, J.S. Binkley, R. Seeger, J.A. Pople, J. Chem. Phys. 72 (1980) 650-654.

[24] M.M. Francl, W.J. Pietro, W.J. Hehre, J.S. Binkley, M.S. Gordon, D.J. DeFrees, J.A. Pople, J. Chem. Phys. 77 (1982) 3654-3665.

[25] M.J. Frisch, J.A. Pople, J.S. Binkley, J. Chem. Phys. 80 (1984) 3265-3269.

[26] J.H. Schachtschneider, F.S. Mortimer, Vibrational Analysis of Polyatomic Molecules. VI. FORTRAN IV Programs for Solving the Vibrational Secular Equation and for the Least-Squares Refinement of Force Constants. Project No. 31450. Structural Interpretation of Spectra. Shell Development Co., Emeryville, CA, 1969.

[27] P. Pulay, G. Fogarasi, F. Pang, J.E. Boggs, J. Am. Chem. Soc. 101 (1979) 2550-2560.

[28] V. Barone, J. Bloino, C.A. Guido, F. Lipparini, Chemical Physics Letters 496 (2010) 157-161.

[29] J. Bloino, V. Barone, J. Chem. Phys. 136 (2012) 124108 (1-15).

[30] V. Barone, M. Biczysko, J. Bloino, Phys. Chem. Chem. Phys. 16 (2014) 1759-1787.

[31] H.G. Korth, M.I. de Heer, P. Mulder, J. Phys. Chem. A 106 (2002) 8779-8789.

[32] A.J. Lopes Jesus, C.M. Nunes, I. Reva, S.M.V. Pinto, R. Fausto, J. Phys. Chem. A 123 (2019) 4396-4405.

[33] T.D. Klots, W.B. Collier, Spectroc. Acta Pt. A-Molec. Biomolec. Spectr. 51 (1995) 1291-1316.

[34] G. Mille, G. Davidovics, J. Chouteau, Comptes Rendus Hebdomadaires Des Seances De L Academie Des Sciences Serie B 274 (1972) 532-535.

[35] J.P. Ferris, F.R. Antonucci, R.W. Trimmer, J. Am. Chem. Soc. 95 (1973) 919-920.

[36] J.P. Ferris, F.R. Antonucci, J. Am. Chem. Soc. 96 (1974) 2014-2019.

[37] C.M. Nunes, S.M.V. Pinto, I. Reva, R. Fausto, Eur. J. Org. Chem. (2016) 4152-4158.

[38] Q. Cao, N. Andrijchenko, A.E. Ahola, A. Domanskaya, M. Räsänen, A. Ermilov, A. Nemukhin, L. Khriachtchev, J. Chem. Phys. 137 (2012) 134305 (1-11).

[39] L. Lapinski, I. Reva, H. Rostkowska, A. Halasa, R. Fausto, M.J. Nowak, J. Phys. Chem. A 117 (2013) 5251-5259.

[40] N. Akai, S. Kudoh, M. Nakata, J. Phys. Chem. A 107 (2003) 3655-3659.

[41] N. Akai, S. Kudoh, M. Takayanagi, M. Nakata, Chem. Phys. Lett. 356 (2002) 133-139.

[42] S. Nanbu, M. Sekine, M. Nakata, J. Phys. Chem. A 115 (2011) 9911-9918.

[43] C.M. Nunes, L. Lapinski, R. Fausto, I. Reva, J. Chem. Phys. 138 (2013) 125101 (1-12).

[44] A. Halasa, L. Lapinski, I. Reva, H. Rostkowska, R. Fausto, M.J. Nowak, J. Phys. Chem. A 118 (2014) 5626-5635.

[45] M. Tsuge, L. Khriachtchev, J. Phys. Chem. A 119 (2015) 2628-2635.

[46] A.J. Lopes Jesus, I. Reva, C. Araujo-Andrade, R. Fausto, J. Chem. Phys. 144 (2016) 124306 (1-9).

[47] R.P. Bell, The Tunnel Effect in Chemistry, Chapman and Hall, London, 1980.

[48] D. Gerbig, P.R. Schreiner, J. Phys. Chem. B 119 (2015) 693-703.

[49] I. Reva, M.J. Nowak, L. Lapinski, R. Fausto, J. Chem. Phys. 136 (2012) 064511 (1-8).

[50] L. Lapinski, I. Reva, H. Rostkowska, R. Fausto, M.J. Nowak, J. Phys. Chem. B 118 (2014) 2831-2841.

UV

cis-OH

NIR

$2\nu(OH)$

H-Tunneling

trans-OH

Ar/N$_2$

N$_2$
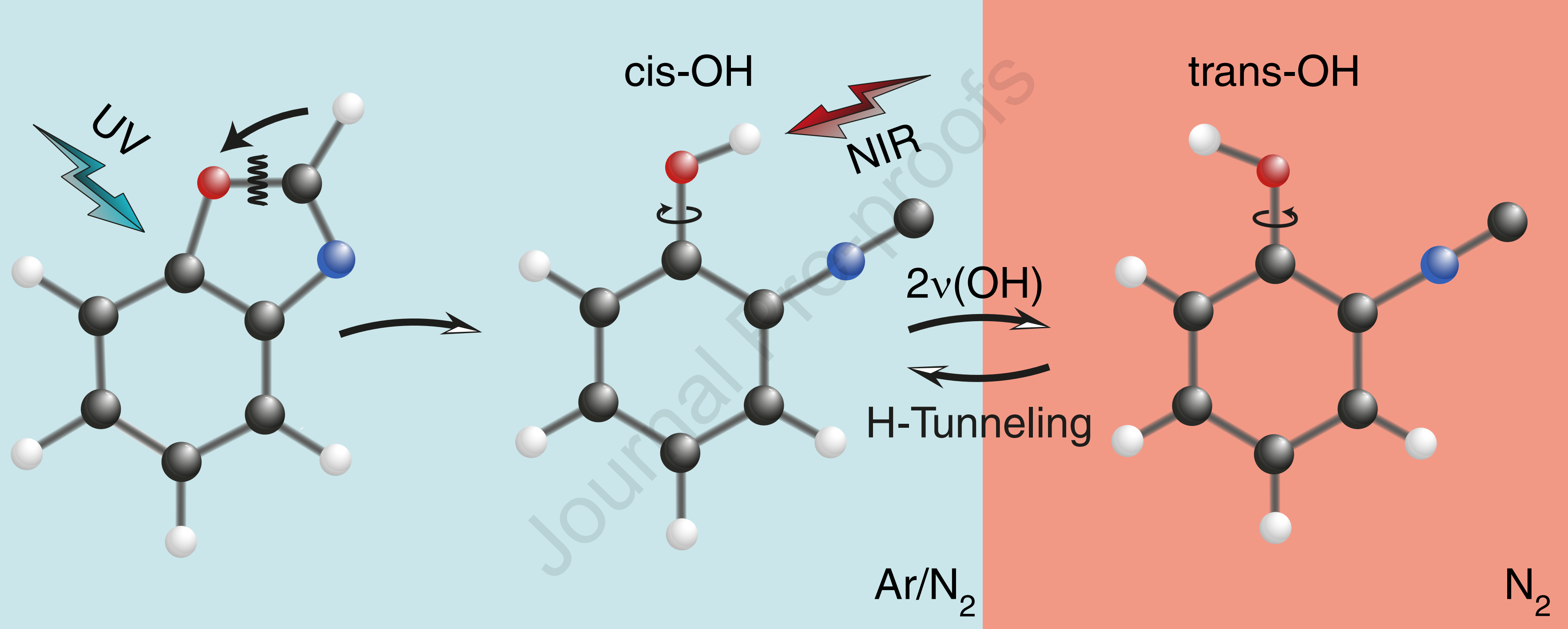
Highlights

UV-irradiation (λ=233 nm) of benzoxazole isolated in Ar or N_2 matrices yields 2-isocyanophenol.
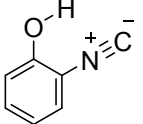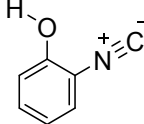
2-isocyanophenol adopts in Ar matrices only the cis conformation, while in N_2 matrices both cis and trans conformers are captured.

Narrowband irradiation at the frequency of the first OH stretching overtone (6986 cm^{-1}) promotes vibrational excitation of the cis conformer, resulting in cis->trans isomerization in N_2 matrices.

The trans conformer decays to the ground state cis form in N_2 matrices in dark, via tunneling.

Structural and vibrational characterization of the two conformers of 2-isocyanophenol is reported.

Table 1. Relative electronic (ΔE_{el}) and zero-point corrected (ΔE_0) energies of **2c** and **2t**, energy barriers for conformational interconversion (ΔΔ$E^{\ddagger}$), and selected structural parameters, computed at two levels of theory.[a]

	2c	**2t**
B3LYP/6-311++G(d,p)		
ΔE_{el}	0.0	11.2
ΔE_0	0.0	10.6
ΔΔ$E^{\ddagger}_{el}$	24.8	13.6
ΔΔ$E^{\ddagger}_0$	22.1	11.5
H···N (Å)	2.311	3.672
O–H···N (degree)	109.8	5.6
MP2/6-311++G(3df,3pd)		
ΔE_{el}	0.0	12.1
ΔE_0	0.0	11.4
ΔΔ$E^{\ddagger}_{el}$	25.4	13.3
ΔΔ$E^{\ddagger}_0$	22.4	11.0
H···N (Å)	2.266	3.640
O–H···N (degree)	110.9	6.0

[a] All energies are in kJ mol⁻¹. Relative energies ΔE_{el} and ΔE_0 are expressed with respect to the most stable **2c** conformer. E_0 = E_{el} + ZPVE (zero-point vibrational energy). The absolute computed values of **2c** are for B3LYP: E_{el} = −399.791881 E_h; E_0 = −399.689588 E_h; and for MP2: E_{el} = −398.908034 E_h; E_0 = −398.805651 E_h. The energy barriers ΔΔ$E^{\ddagger}_{el}$ and ΔΔ$E^{\ddagger}_0$ are without and with the ZPVE contribution, respectively. They are measured from the respective local minimum (either **2c** or **2t**).
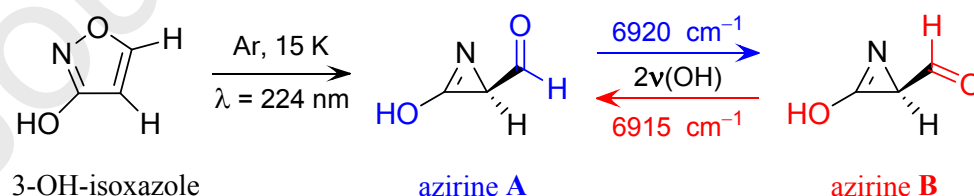

Fig. 1. UV-induced generation of elusive 3-hydroxy-2-formyl-2*H*-azirine (briefly, "azirine") from 3-hydroxy-isoxazole (briefly, "3-OH-isoxazole") in an Ar matrix at 15 K, and subsequent conformational control of the formyl group in the azirine by NIR-induced narrowband vibrational excitation of the first OH stretching overtones, 2v(OH), of the respective azirine conformers, **A** and **B**.
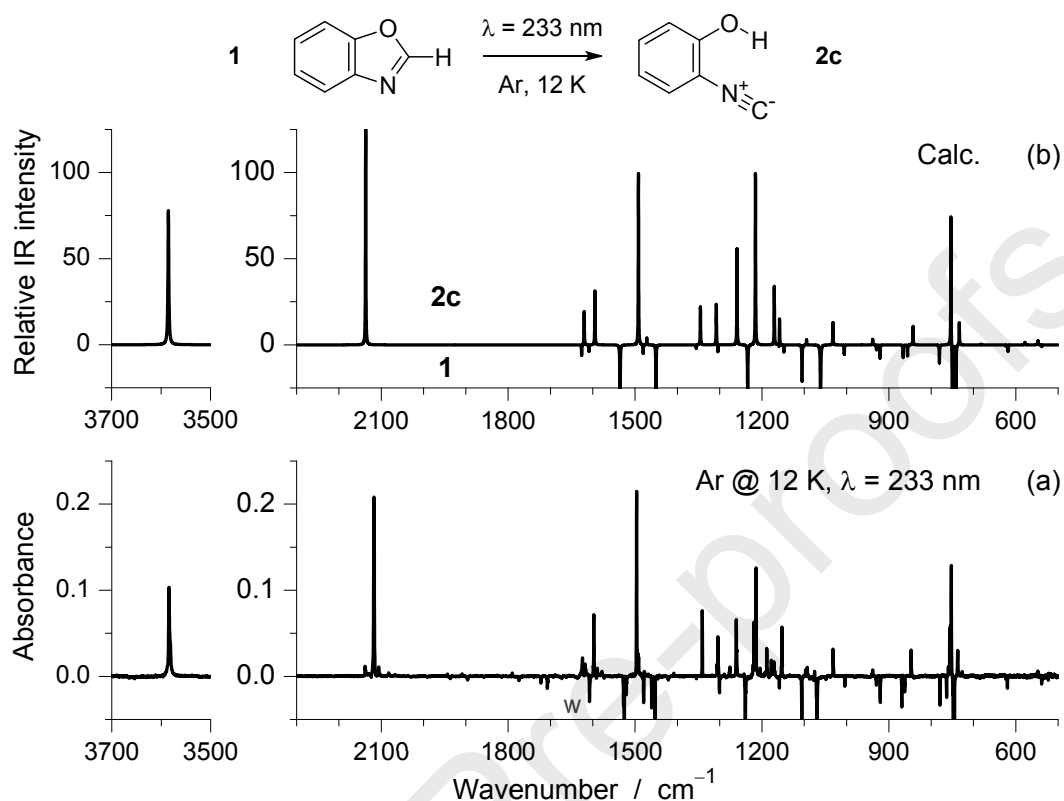
Fig. 2. UV-generation of 2-isocyanophenol **2** in an Ar matrix at 12 K: (a) Experimental IR spectrum showing changes after irradiation at λ = 233 nm (18 min, ~10 mW) of matrix-isolated benzoxazole **1**, obtained as the spectrum of the irradiated sample minus the spectrum of the sample before irradiation. The growing bands are due to photoproducts. The decreasing bands are due to **1** and are truncated. The band marked with "w" is due to matrix-isolated water monomers; (b) Theoretical difference IR spectrum assuming quantitative transformation of **1** into **2c**, obtained as the spectrum of **2c** minus the spectrum of **1** (negative bands, truncated). In simulations, an fwhm of 1 cm^{-1} was used (see the computational section for the frequency scaling details).

17
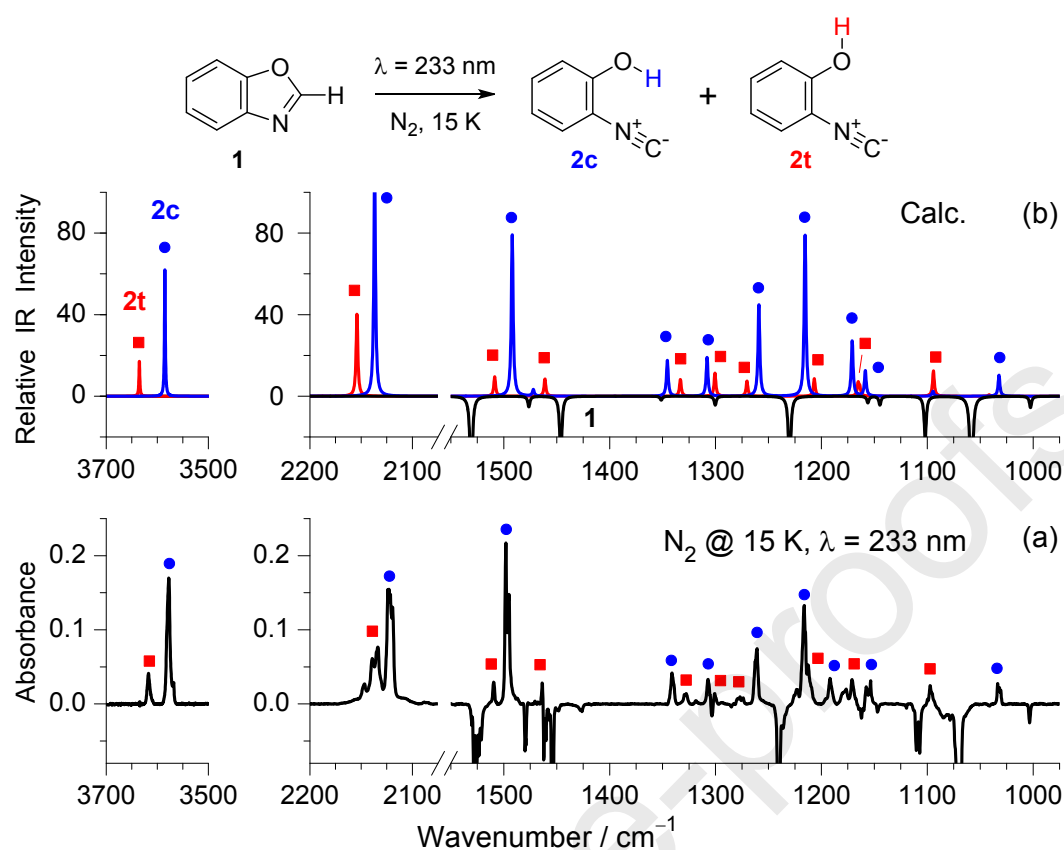
Fig. 3. UV-generation of two forms of 2-isocyanophenol **2** in an N₂ matrix at 15 K: (a) Experimental IR spectrum showing changes after irradiation at λ = 233 nm (~1 h, ~10 mW) of matrix-isolated benzoxazole **1**, obtained as spectrum of the irradiated sample minus spectrum of the sample before irradiation. The growing bands are due to photoproducts. The decreasing bands are due to **1** and are truncated; (b) Simulated theoretical IR spectra of **2c** (blue line, blue circles), **2t** (red line, red squares) and of **1** (black, negative, truncated). In simulations, the computed infrared intensities of **2c**, **2t**, and **1** were scaled by 0.8, 0.2, and (−1) respectively, and an fwhm of 2 cm⁻¹ was used (see the computational section for the frequency scaling details).
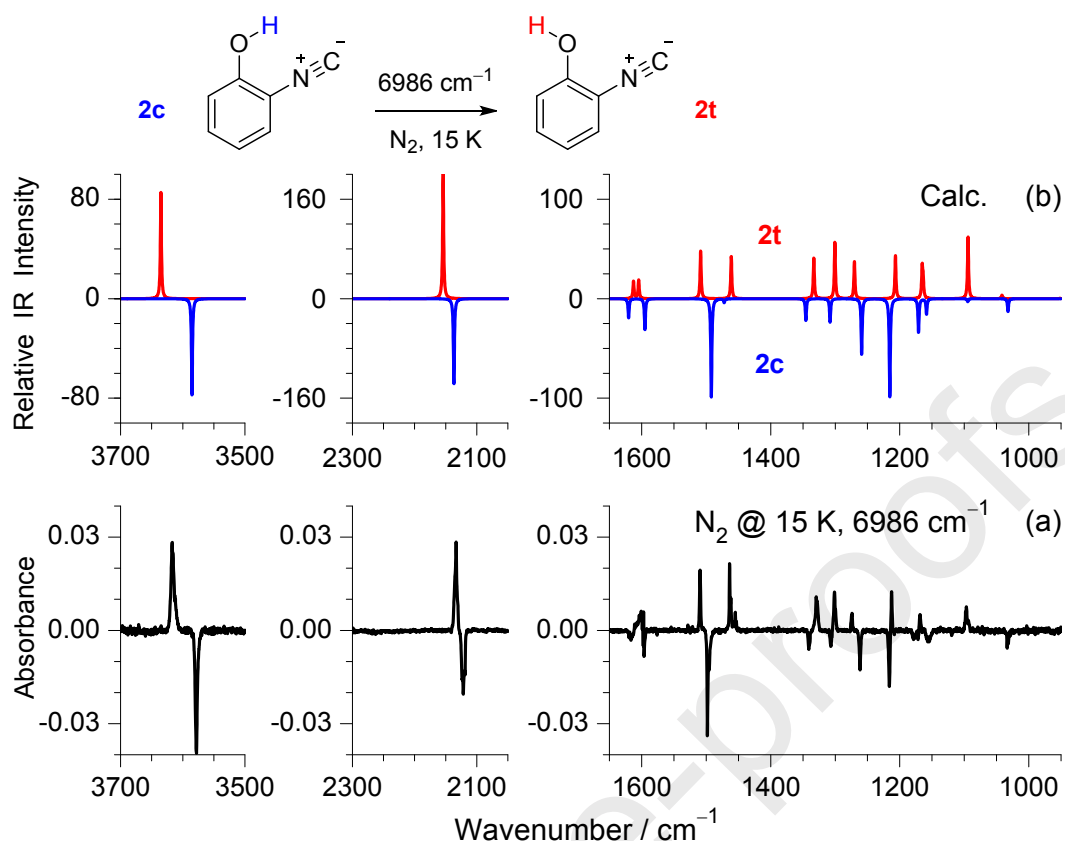
Fig. 4. Conformational **2c** → **2t** isomerization in an N$_2$ matrix at 15 K induced by vibrational excitation of **2c**. (a) Experimental IR spectrum showing changes after NIR-irradiation at 6986 cm^{-1} (~1.5 h, ~70 mW) of the sample that was earlier UV-irradiated at λ = 233 nm, obtained as the spectrum of the NIR-irradiated sample minus the spectrum of the sample before the NIR irradiation. The growing bands are positive and the decreasing are negative; (b) Simulated theoretical IR spectra of **2c** (blue line, negative) and **2t** (red line, positive). In simulations, the computed infrared intensities of **2c** and **2t** were multiplied by (−1) and (+1), respectively, and an fwhm of 2 cm^{-1} was used (see the computational section for the frequency scaling details).

19
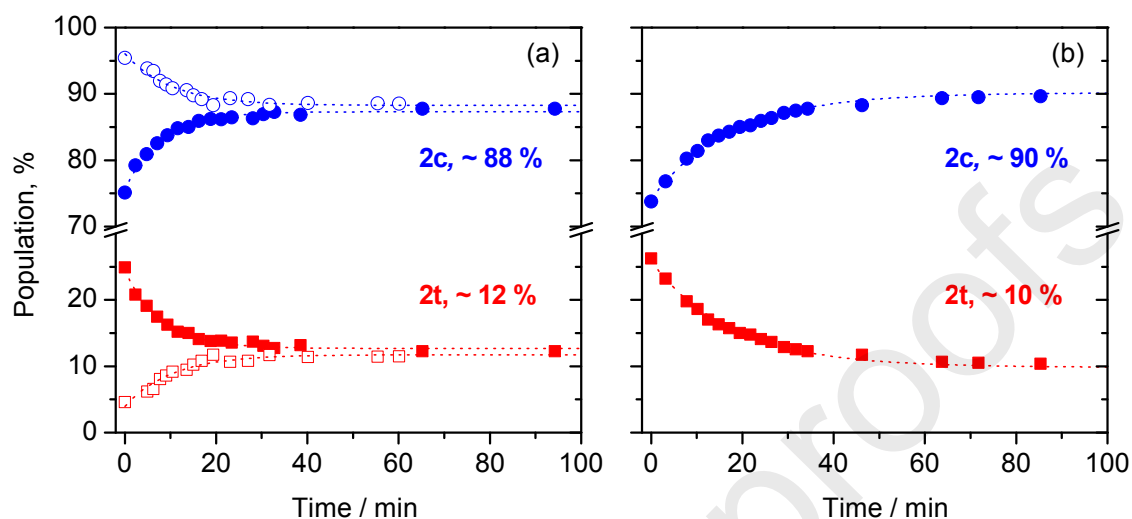
Fig. 5. Time evolution of the population of **2c** (circles) and **2t** (squares) forms during the exposure of matrix-isolated **2** (N_2, 15 K) to (a) unfiltered and (b) filtered (blocked above ~ 2200 cm^{-1}) broadband IR light emitted by the spectrometer source. The **2c** : **2t** conformational ratio at the start of the kinetic measurements was 75 : 25 (solid symbols) or 95 : 5 (open symbols). The populations were estimated from the integrated absorbance of the bands centered at 1341 cm^{-1} (**2c**) and 1329 cm^{-1} (**2t**), divided by their respective calculated IR intensities (see Tables S3 and S4). Dotted traces represent the best exponential fits to the experimental data. For all fits $R^2 = 0.98{-}0.99$.
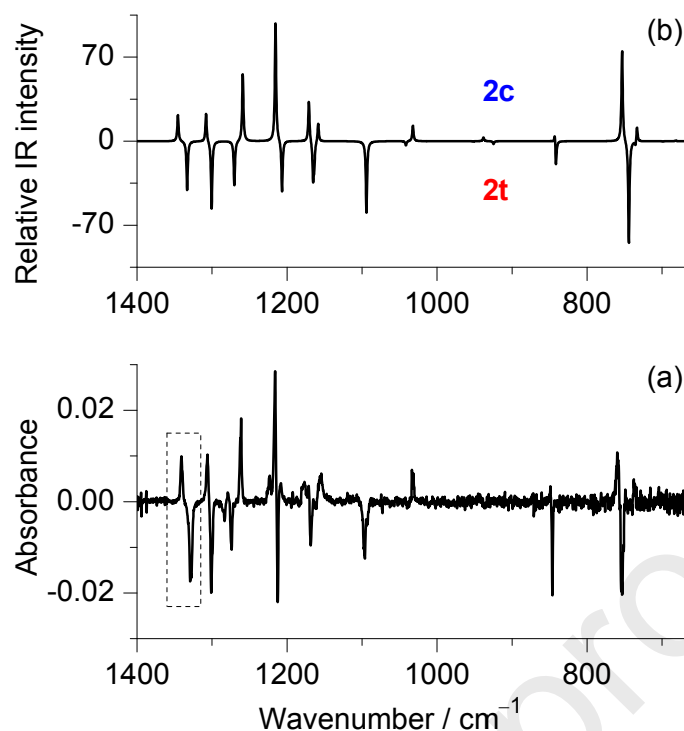
Fig. 6. Spontaneous **2t** → **2c** isomerization in dark. (a) Experimental IR spectrum showing changes after keeping matrix-isolated **2** (N$_2$, 11 K) in dark for 23 h, obtained as the spectrum at the end of monitoring (after 23 h) minus that recorded immediately after NIR irradiations at 6986 cm^{-1}, which corresponds to the start of monitoring. The growing bands are positive and the decreasing are negative. During the spectra acquisition, a longpass filter, only transmitting below 2200 cm^{-1}, was placed between the sample and the spectrometer source. Between measurements, a metal plate was used to completely block the spectrometer beam. For the 2200-1300 cm^{-1} range, see Fig. S6. The dashed rectangle designates a fragment of spectrum shown in Fig.7; (b) Theoretical difference IR spectrum assuming quantitative transformation of **2t** into **2c**, obtained as the spectrum of **2c** minus the spectrum of **2t** (negative bands). In simulations, an fwhm of 2 cm^{-1} was used (see the computational section for the frequency scaling details).

21
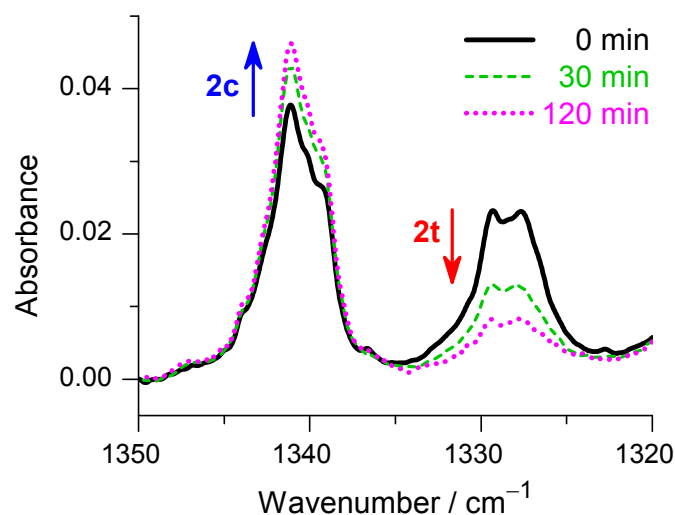
Fig. 7. Fragments of infrared spectra of **2** isolated in N_2 matrix at 11 K, showing the decay of **2t** and the simultaneous growth of **2c** in the dark. The populations of **2c** and **2t** were estimated from the integrated absorbance of the bands centered at 1341 cm^{-1} and 1329 cm^{-1}, divided by their respective calculated IR intensities (see Tables S3 and S4). The solid (black) trace represents the sample enriched with **2t** by preceding NIR irradiations at 6986 cm^{-1}, and corresponds to the start of monitoring (t= 0 min). The spectra shown as green (dashed) and pink (dotted) were collected after 30 and 120 min of monitoring, respectively. The sample was kept in the dark during the decay, except for the recording IR spectra, when a longpass cut-off filter transmitting only below 2200 cm^{-1} was used.

Author Contribution Statement

A. J. Lopes Jesus: Writing- Original draft preparation, Formal analysis;
Igor Reva: Writing - Original draft preparation, Writing - Review & Editing, Supervision;
Cláudio M. Nunes: Investigation, Conceptualization;
José P. L. Roque: Visualization, Formal analysis;
Sandra M. V. Pinto: Investigation;
R. Fausto: Funding acquisition, Resources, Supervision.

Declaration of interests

24

☒ The authors declare that they have no known competing financial interests or personal relationships that could have appeared to influence the work reported in this paper.

☐The authors declare the following financial interests/personal relationships which may be considered as potential competing interests:

Declaration of interests